Originalarbeit

Berg Huettenmaenn Monatsh (2022) Vol. 167 (11): 542–545
https://doi.org/10.1007/s00501-022-01294-4

BHM Berg- und Hüttenmännische Monatshefte

Effect of Si and Al on Retained Austenite Stabilization during Q&P and Galvannealing Process

Matthias Wallner[1,2], Katharina Steineder[3], Reinhold Schneider[1], and Christof Sommitsch[2]

[1]Department for Materials Technology, Univ. of Appl. Sciences Upper Austria, Wels, Austria
[2]Institute of Material Science, Joining and Forming, Graz Univ. of Tech., Graz, Austria
[3]Research & Development and Innovation, voestalpine Stahl GmbH, Linz, Austria

Received September 1, 2022; accepted October 7, 2022; published online November 10, 2022

Abstract: The present contribution concentrates on the different effects of Si and Al on the carbide precipitation and austenite decomposition during the Q&P-process and an additional galvannealing treatment of up to 560 °C. These effects have been investigated by dilatometry (derivation of relative length change) and differential scanning calorimetry (heat flow) during tempering. It was possible to show the beneficial effect of Si on retarding the carbide precipitation in tempered martensite and thereby the ability to stabilize higher amounts of retained austenite compared to Al. Furthermore, the effect on retained austenite decomposition during Q&P and subsequent galvannealing could be demonstrated. Here, Al has the benefit to increase the thermal stability of austenite during galvannealing.

Keywords: Q&P-process, Carbide precipitation, Dilatometry, Thermal austenite stability, Galvannealing

Einfluss von Si und Al auf die Restaustenitstabilisierung während des Q&P- und Galvannealing-Prozesses

Zusammenfassung: Der vorliegende Beitrag konzentriert sich auf die unterschiedlichen Auswirkungen von Si und Al auf die Karbidausscheidung und Austenitzersetzung während des Q&P-Prozesses mit anschließendem Galvannealing bis zu 560 °C. Diese Effekte wurden mittels Dilatometrie (Ableitung der relativen Längenänderung) und Differentialkalorimetrie (Wärmemenge) während des Anlassens untersucht. Es konnte eine positive Wirkung von Si auf die Verzögerung der Karbidausscheidung im angelassenen Martensit und damit die Fähigkeit zur Stabilisierung höherer Mengen an Restaustenit im Vergleich zu Al nachgewiesen werden. Darüber hinaus konnte die Auswirkung auf die Zersetzung von Restaustenit während des Q&P und des anschließenden Galvannealens gezeigt werden. Hier hat Al den Vorteil, dass es die thermische Stabilität von Austenit während des Galvannealens erhöht.

Schlüsselwörter: Q&P-Verfahren, Karbidausscheidung, Dilatometrie, Thermische Austenitstabilität, Galvannealing

1. Introduction

Using quenching and partitioning (Q&P) heat treatment, steels with not only high products of strength and elongation [1], but also enhanced bendability can be produced. These steels are increasingly used in the automotive industry to improve crash safety and the lightweight potential of vehicles equally. Commonly these steels contain high amounts of Si for stabilizing high fractions of retained austenite (RA), necessary for the transformation induced plasticity (TRIP) effect. With regard to the hot dip galvanizing and galvannealing process, these high Si contents cause several problems, such as in wettability and weldability. Therefore, Si is increasingly replaced by Al. So far most of the studies have focused on the effect of Si on the carbide precipitation and RA decomposition during the Q&P process. In this study, the impact of Al compared to Si as an alloying element, during a conventional Q&P process and additional galvannealing heat treatment, was investigated. The main focus was on carbide precipitation in martensite and retained austenite decomposition.

2. Experimental

Two different medium-Mn-steels, one Si-alloyed steel (Fe-0.2C-4Mn-1.5Si in wt.%) and one Al-alloyed steel (Fe-0.2C-4Mn-1.5Al in wt.%), were produced under laboratory conditions. Subsequently, the material was hot

M. Wallner (✉)
Department for Materials Technology,
Univ. of Appl. Sciences Upper Austria,
Wels, Austria
matthias.wallner@fh-wels.at

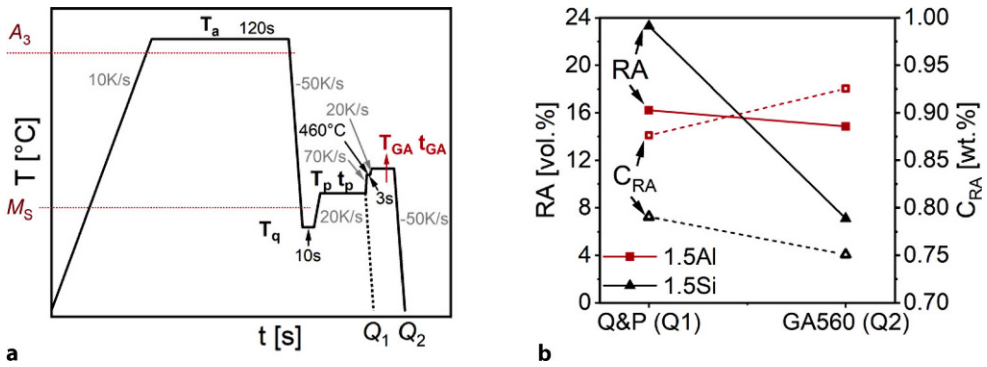

Fig. 1: **a** Schematic representation of the quenching and partitioning (Q&P) process followed by a galvannealing (GA) process; **b** XRD-measured RA-fraction and C-content in RA for the steels Fe-0.2C-4 Mn-1.5Si and Fe-0.2C-4 Mn-1.5Al in condition Q1 & Q2

rolled to a thickness of 4 mm, followed by tempering at 550 °C for 16 h to provide cold rollability. After cold rolling to a thickness of 1 mm, the steels were Q&P heat-treated, shown in Fig. 1, using a Bähr 805 A/D dilatometer. Samples ($4 \times 1 \times 10\,mm^3$) were fully austenitized (T_a) at 850 °C for the Si-steel and 900 °C for the Al-steel. Afterwards, samples were quenched to quenching temperatures (T_q) of 230 °C for Si-steel and 270 °C for Al-steel respectively, which resulted in 60% martensite (α'_1) in both steels. After a short holding time at T_q, samples were heated to a partitioning temperature (T_p) of 400 °C, held for 40 s, and cooled to room temperature (Q_1). To investigate the influence of an additional galvannealing (GA) treatment, further samples were treated with the same Q&P cycle, but after partitioning, were reheated first to 460 °C (simulating the liquid zinc bath) and then to a galvannealing temperature (T_{GA}) of 560 °C for 20 s. Amount and lattice parameter of RA were measured by X-ray diffraction (XRD). C-content in RA was calculated according to the equation in [2]. The microstructure was investigated by scanning electron microscopy (SEM) and electron backscatter diffraction (EBSD). Furthermore, as quenched samples and samples with defined amounts of α'_1 were continuously tempered with 10 K/min by dilatometry (DIL) and differential scanning calorimetry (DSC) on a Mettler Toledo DSC 3. Thereby derivation of relative length change (dl/dT) and heat flow was evaluated to determine the different effects of Si and Al on carbide precipitation and RA decomposition.

3. Results and Discussion

3.1 Martensite Tempering Effects during the Q&P Process

After the Q&P cycle (Q_1) with chosen T_q, the highest RA-fractions (Fig. 1b) were stabilized after a partitioning at 400 °C for 40 s. The corresponding microstructure (Fig. 2a,b) consists of around 60% α'_1 for both steels. The Al-steel shows a significantly larger prior austenite grain size (PAGS). RA, which is around 23% for the Si-steel and 16% for Al-steel, has a lathlike shape, as shown in EBSD-phase mapping, and is located between the α'_1-needles and at the prior austenite grain boundaries. Some austenite, which was not stabilized sufficiently, transformed to fresh martensite α'_2 during quenching to room temperature (dark areas in phase mapping). The amount of RA, which can be stabilized by Q&P, depends, beside the amount of initial α'_1, especially on the free carbon-content, which can be partitioned from α'_1 to the RA. Carbides formed in α'_1 act as carbon sinks and reduce the C-partitioning potential. The higher RA-fraction of the Si-steel can thereby be mainly explained by the different effect of Si and Al on the carbide precipitation kinetics during α'_1 tempering. Those are the focus of the DSC/DIL α'_1 tempering tests.

Fig. 2c shows the characteristic tempering stages starting from an almost fully martensitic microstructure (~3–4% RA) of both steels. Here the typical tempering steps, also shown by [3] and [4], express themselves differently in heat flow and length change. At lower temperatures of around

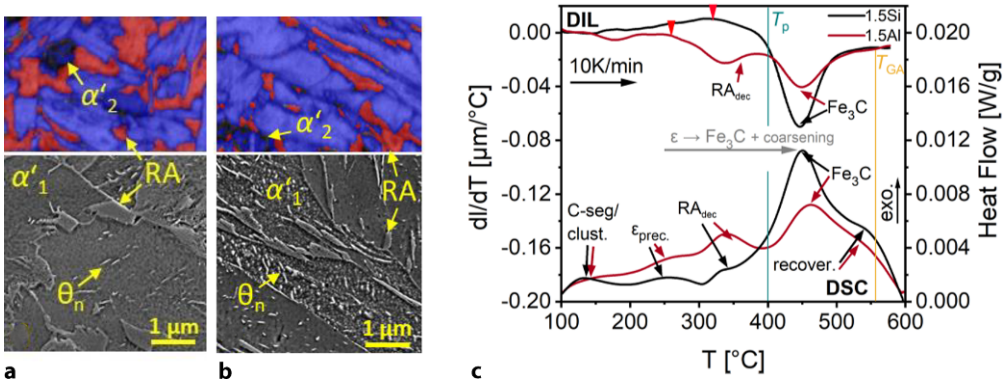

Fig. 2: SEM- and EBSD-combined band slope & phase map images (red; fcc; blue: bcc) images of **a** Fe-0.2C-4 Mn-1.5Si and **b** Fe-0.2C-4 Mn-1.5Al after Q&*P*: **c** derivation of rel. length change (DIL) and heat flow curve (DSC) during martensite tempering of both steels

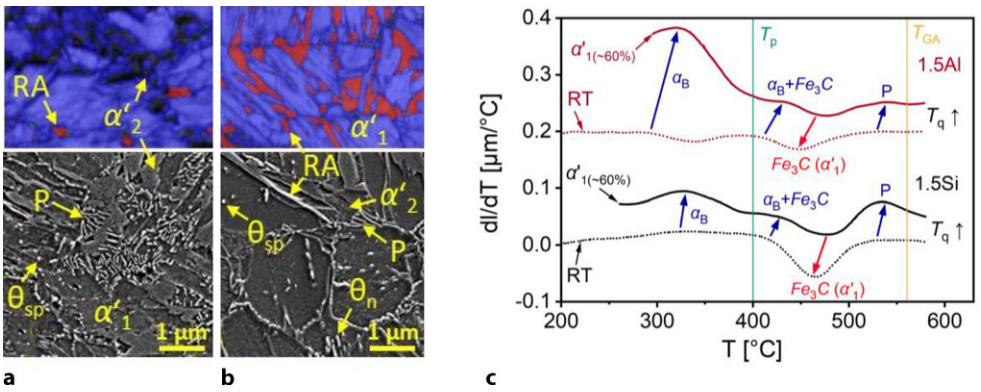

Fig. 3: SEM and EBSD-combined band slope and phase map (red; fcc; blue: bcc) images of **a** Fe-0.2C-4Mn-1.5Si and **b** Fe-0.2C-4Mn-1.5Al after Q&P + GA: **c** derivation of relative length change (DIL) and heat flow curve (DSC) during tempering of both steels with initially 40% RA

140 °C, small exothermal peaks can be found in the heat flow curve attributed to C segregations and C clustering. At 260 °C, transition-carbides, like ε/η-carbides, start to precipitate, which happens under paraequilibrium conditions. According to [5], Si-content has no noticeable influence on this precipitation, whereby Al is suggested to even promote the formation of transition carbides. With increasing temperature, they gradually coarsen and transform into Fe_3C (cementite). This effect is especially pronounced for the Al-steel as a contraction in dilatation. The start temperature of contraction of about 260 °C (red triangle) is lower for the Al-steel compared to the Si-steel, were the dilatation starts to decrease not until around 330 °C. According to [5] this can be explained to the limited effect of Al on the transition of transition carbides into cementite at temperatures lower than 400 °C.

Focusing on the SEM-images in Fig. 2a, b, this theory can be confirmed as only some fine separated needle shaped carbides (θ_n) can be found in the Si-steel after Q&P process. In the Al-steel, high amounts of coarse θ_n appear, which explains the lower amount of RA. At the partitioning temperature of 400 °C, the carbides can be assumed to be a mixture of transition carbides and cementite. The next tempering step is the RA decomposition into bcc + carbides (bainite), which is expressed by an increased heat flow. A positive dilatation could only be observed for the Al steel. At even higher temperatures of above 450 °C, Fe_3C precipitation and coarsening occur. As more carbides have already precipitated and transformed into cementite at lower temperatures in the Al steel, this reaction is less pronounced compared to Si steel. At temperatures higher than 550 °C, a further exothermal peak can be found, which can be attributed to recovery phenomena. The overall higher C content in RA for the Al steel after Q_1 (Fig. 1b) contradicts its pronounced carbide precipitation behaviour. This can be explained by the lower amount of RA of the Al steel (16%) compared to the Si steel (23%). A higher content of C is stabilizing the RA of the Al steel, but in absolute terms, there is more C partitioned to the RA of the Si steel.

3.2 Austenite Decomposition during GA

Due to an additional GA thermal cycle after partitioning, at the relatively high temperature of 560 °C, RA decreases significantly to 7% in the Si steel (Fig. 1b), while it almost remains constant with around 15% in the Al steel. As shown in Fig. 3a, the larger RA islands of the Si steel have been decomposed into bcc + carbides (pearlite) and some α'_2 (darker areas in phase map) has formed. For the Al steel (Fig. 3b), large RA areas still can be found (EBSD map).

The reactions occurring during constant heating from an initial microstructure of 60% α'_1 and 40% remaining austenite are shown in Fig. 3c. Focusing on the two solid lines for 60% α'_1, a significant expansion can be found directly after quenching to Tq up to about 350 °C. This expansion is related to the formation of bainitic ferrite (carbide free bainite) αB and is significantly stronger for the Al steel. This αB can, as long as it is carbide free, further increase RA stability and C content due to additional C partitioning. At temperatures above 400 °C, a slight increase in dilatation occurs due to a decomposition of austenite into bainite ($\alpha_B + Fe_3C$), interacting with a contraction due to Fe_3C formation and coarsening in α'_1. As the amount of α'_1 is lower than after quenching to room temperature (dotted line, RT), this effect is less pronounced. At around 550 °C, the significant expansion for the Si steel results from the decomposition of RA into pearlite (P), as seen in Fig. 3a,b. In contrast, the Al steel exhibits only a slight increase in relative length change due to pearlite formation, which correlates well with the microstructure in Fig. 3b. RA fraction and C content in RA for the Al steel remains almost constant during annealing at 560 °C, whereas it strongly decreases due to carbon depleting effect of pearlite formation in the Si steel. After GA treatment at 560 °C, which is higher than the Fe_3C peak in Fig. 2, carbides are assumed to be exclusively Fe_3C. Most of the carbides in the Si steel are spheroidized (θ_{sp}) and accumulate at the PAGB. In the Al steel only small amounts of θ_{sp} can be found, but more needle shaped θ_n are still present.

4. Conclusions

At temperatures of around 400 °C, a significantly higher amount of coarse carbides precipitate in tempered martensite, limiting C partitioning and thereby the amount of retained austenite, when alloying a medium-Mn-Q&P steel with Al instead of Si.

Furthermore, Al stimulates, compared to Si, an increased bainitic ferrite formation at partitioning temperature, but significantly retards the austenite to pearlite decomposition and carbide coarsening. Both effects have a positive impact on RA retention during a galvannealing treatment.

Acknowledgements. The authors sincerely acknowledge the support of the Austrian Research Promotion Agency (FFG) related to the frontrunner project No. 860188 "Upscaling of medium Mn-TRIP steels".

Funding. Open access funding provided by University of Applied Sciences Upper Austria.

References

1. Speer, J., Matlock, D., De Cooman, B.C.: Carbon partitioning into Austenite after Martensite transformation. Acta Mater. **51**, 2611–2622 (2003)
2. van Dijk, N.H., Butt, A.M., Zhao, L.: Thermal stability of retained austenite in TRIP steels studied by synchrotron X-ray diffraction during cooling. Acta Mater. **53**, 5439–5447 (2005)
3. De Moor, E., Lacroix, S., Samek, L., et al.: Dilatometric study of the quench and partitioning process. In: 3rd Int. Conf. of Adv. Struc. Steels Gyeongju, Korea (2006)
4. Vieweg, A., Povoden-Karadeniz, E., Ressel, G.: Phase evolution and carbon redistribution during continuous tempering of martensite studied with high resolution techniques. Mater. Des. **136**, 214–222 (2017)
5. Zhu, K., Shi, H., Chen, H., Jung, C.: Effect of Al on martensite tempering: comparison with Si. J. Mater. Sci. **53**, 6951–6967 (2018)